Hsp47 promotes cancer metastasis by enhancing collagen-dependent cancer cell-platelet interaction

Gaofeng Xiong[a,b], Jie Chen[a,b], Guoying Zhang[c], Shike Wang[a,b], Kunito Kawasaki[d], Jieqing Zhu[a,b], Yan Zhang[c], Kazuhiro Nagata[d], Zhenyu Li[c], Binhua P. Zhou[a,e], and Ren Xu[a,b,1]

[a]Markey Cancer Center, University of Kentucky, Lexington, KY 40536; [b]Department of Pharmacology and Nutritional Sciences, University of Kentucky, Lexington, KY 40536; [c]Division of Cardiovascular Medicine, Department of Internal Medicine, University of Kentucky, Lexington, KY 40536; [d]Department of Molecular and Cellular Biology, Kyoto Sangyo University, Kyoto 603-8555, Japan; and [e]Department of Molecular and Cellular Biochemistry, University of Kentucky, Lexington, KY 40536

Edited by Joan S. Brugge, Harvard Medical School, Boston, MA, and approved January 8, 2020 (received for review July 11, 2019)

Increased expression of extracellular matrix (ECM) proteins in circulating tumor cells (CTCs) suggests potential function of cancer cell-produced ECM in initiation of cancer cell colonization. Here, we showed that collagen and heat shock protein 47 (Hsp47), a chaperone facilitating collagen secretion and deposition, were highly expressed during the epithelial-mesenchymal transition (EMT) and in CTCs. Hsp47 expression induced mesenchymal phenotypes in mammary epithelial cells (MECs), enhanced platelet recruitment, and promoted lung retention and colonization of cancer cells. Platelet depletion in vivo abolished Hsp47-induced cancer cell retention in the lung, suggesting that Hsp47 promotes cancer cell colonization by enhancing cancer cell–platelet interaction. Using rescue experiments and functional blocking antibodies, we identified type I collagen as the key mediator of Hsp47-induced cancer cell–platelet interaction. We also found that Hsp47-dependent collagen deposition and platelet recruitment facilitated cancer cell clustering and extravasation in vitro. By analyzing DNA/RNA sequencing data generated from human breast cancer tissues, we showed that gene amplification and increased expression of Hsp47 were associated with cancer metastasis. These results suggest that targeting the Hsp47/collagen axis is a promising strategy to block cancer cell–platelet interaction and cancer colonization in secondary organs.

extracellular matrix | cancer metastasis | epithelial-mesenchymal transition | breast cancer | circulating tumor cell

Metastasis is the cause of 90% of cancer-related deaths in breast cancer patients (1). Therefore, understanding how cancer cells spread and colonize distant organs is crucial for identifying novel strategies to halt cancer progression and improve cancer treatment. Cancer metastasis is a multistep process involved in detachment from the primary tumor, survival in circulation, colonization, and formation of macrometastases in secondary organs (2). Once cancer cells enter the circulation system, they encounter a variety of environmental stressors, such as detachment from the extracellular matrix (ECM) substrate, shear force, oxidative stress, and attack from immune cells (3, 4). Only a small number of cancer cells can survive in circulation and establish metastasis lesions (5, 6). How circulating tumor cells (CTCs) overcome environmental stress and initiate this colonization is not clearly understood.

The epithelial-mesenchymal transition (EMT) is an important cellular event that contributes to cancer metastasis (7, 8). The EMT process, characterized by the loss of epithelial characteristics and acquisition of mesenchymal phenotypes, is induced by a number of cytokine and transcription factors, including transforming growth factor (TGF)-β, Twist, Snail, and Slug, during tumor progression (9). The EMT enhances cancer cell migration and invasion and also promotes cancer cell colonization at distant organs (9, 10). Single-cell sequencing data has demonstrated that CTCs exhibit increased expression of EMT-related genes (11, 12). It has been proposed that activation of the EMT program enhances cancer cell survival in circulation and facilitates cancer cell recolonization at the distal sites; however, the exact function of mesenchymal phenotypes in CTCs remains to be determined.

ECM is a determinant in the tumor microenvironment that controls cancer development and progression (13, 14). Stromal cells, such as cancer associate fibroblasts (CAFs), are considered the major source of ECM in tumor tissue; interestingly, cancer cells also deposit a significant quantity of ECM proteins (15–20). Cancer cell-produced ECM molecules, such as tenascin-C, are the important components of metastatic niches and facilitate cancer cell colonization during metastasis (15, 18, 19). We recently identified heat shock protein 47 (Hsp47) as a hub of the ECM transcription network (20, 21). Binding of Hsp47 to collagen facilitates collagen secretion and deposition (22). The Hsp47 gene locates at 11q13, a region often amplified in cancer (23). In addition, increased Hsp47 expression is associated with advanced cancer stage, shortened recurrence-free survival, and metastasis (20, 24). This evidence suggests that Hsp47 may contribute to cancer progression.

In this study, we show that expression of Hsp47 and collagen are induced during the EMT. Hsp47 expression enhances cancer cell–platelet interaction by inducing collagen deposition in breast cancer cells and subsequently promotes cancer cell clustering and colonization at distant sites. These results reveal the molecular mechanism by which the EMT enhances cancer cell–platelet

Significance

Cancer cell–platelet interaction is crucial for cancer metastasis; however, how this interaction is regulated remains largely unknown. We have identified Hsp47 as an EMT inducer and showed that Hsp47 and its dependent collagen secretion enhanced cancer cell–platelet interaction. Importantly, Hsp47-induced cancer cell–platelet interaction enhanced cancer cell clustering, which is crucial for cancer cell colonization at distant sites. We also found that Hsp47 gene amplification and expression were associated with breast cancer metastasis. These results reveal a link between the Hsp47/collagen axis and platelet recruitment, and provide additional insight into how mesenchymal phenotypes in cancer cells contribute to breast cancer metastasis.

Author contributions: G.X. and R.X. designed research; G.X., J.C., G.Z., S.W., J.Z., Y.Z., Z.L., and R.X. performed research; K.K. and K.N. contributed new reagents/analytic tools; G.X., J.C., G.Z., Z.L., B.P.Z., and R.X. analyzed data; and G.X. and R.X. wrote the paper.

The authors declare no competing interest.

This article is a PNAS Direct Submission.

Data deposition: Microarray data have been deposited in the Gene Expression Omnibus (GEO) database, https://www.ncbi.nlm.nih.gov/geo (accession no GSE143349).

[1]To whom correspondence may be addressed. Email: ren.xu2010@uky.edu.

This article contains supporting information online at https://www.pnas.org/lookup/suppl/doi:10.1073/pnas.1911951117/-/DCSupplemental.

First published February 3, 2020.

interaction, and identifies a previously unreported function of the Hsp47/collagen axis in breast cancer metastasis.

Results

Hsp47 Expression Promotes the EMT and Cancer Cell Stemness. ECM remodeling is necessary for cancer development and progression (13, 14). We previously identified an ECM transcriptional network in human breast cancer tissues, the expression of which is induced during cancer development (20). Hsp47, one hub of the ECM network, promotes tumor invasion and collagen deposition in the xenograft model (20). The EMT is accompanied by ECM remodeling and cell invasion; therefore, we asked whether expression of Hsp47 and ECM network genes are associated with the EMT process. By analyzing gene expression profiles generated from mammary epithelial cells (MECs) that had undergone the EMT (Twist- or Snail-induced), we found that ECM network genes, such as COL1A1, COL1A2, and COL4A1, were induced during the EMT process (Fig. 1*A*). Transcription and protein expression of Hsp47 were also significantly increased in Twist- or Snail-induced EMT cells (Fig. 1 *B–D* and *SI Appendix*, Fig. S1 *A–C*).

To determine whether Hsp47 expression is functionally important for the EMT process, we isolated primary MECs from MMTV-Cre:Hsp47$^{+/lox}$ and MMTV-Cre:Hsp47$^{lox/lox}$ mice and cultured them on plastic. We found that Hsp47-positive MECs acquired mesenchymal phenotypes after 4 to 5 d. Interestingly, Hsp47$^{-/-}$ MECs maintained their epithelial phenotypes and E-cadherin expression much longer than Hsp47-positive cells (Fig. 1*E*). Western blot analysis data further confirmed that compared with Hsp47-positive cells, Hsp47$^{-/-}$ epithelial cells had higher expression levels of the epithelial cell marker E-cadherin and lower expression levels of mesenchymal markers such as N-cadherin and vimentin (Fig. 1*F*). Silence of Hsp47 in HMLE cells also inhibited TGF-β–induced EMT (*SI Appendix*, Fig. S1 *D* and *E*). Interestingly, the addition of exogenous type I collagen only partially rescued EMT phenotypes in Hsp47-silenced cells (*SI Appendix*, Fig. S1 *D* and *E*), suggesting that other Hsp47 substrates also contribute to this process. In the gain-of function experiments, introducing exogenous Hsp47 in MCF10A and HMLE cells increased protein levels of N-cadherin, vimentin, and Snail and reduced expression of E-cadherin (Fig. 1*G* and *SI Appendix*, Fig. S1*F*). Hsp47 expression in MCF10A cells also enhanced EMT phenotypes, such as cell invasion and migration (*SI Appendix*, Fig. S1 *G* and *H*).

Importantly, by analyzing gene expression profiles in The Cancer Genome Atlas (TCGA) human breast cancer datasets, we found that mRNA levels of Hsp47 (SERPINH1) significantly correlated with the levels of EMT regulators and EMT markers, including TWIST1, SNAI1, FN1, and CDH2 (Fig. 1 *H–J* and *SI Appendix*, Fig. S1*I*). Therefore, Hsp47 expression may contribute to activation of the EMT program during breast cancer progression.

Tumor-initiating cells (TICs) are cancer cells with stem cell characteristics that drive cancer development and metastasis. The EMT is a cellular event that enhances cancer cell stemness (7, 8). By comparing gene expression profiles generated from a TIC-enriched tumorsphere and matched primary tumor cells (25), we found that transcription of the Hsp47 gene and many collagen genes was induced in tumorspheres (Fig. 1 *K* and *L*). Results from the tumorsphere formation assay showed that silencing Hsp47 significantly reduced tumorsphere formation efficiency in triple-negative breast cancer (TNBC) cells (Fig. 1*M*). Knockdown of Hsp47 also inhibited colony formation of MDA-MB-231 cells (*SI Appendix*, Fig. S1 *J–M*). These results suggest that Hsp47 expression enhances cancer cell stemness.

Hsp47 Expression Enhances Cancer Cell Colonization and Metastasis. Activation of the EMT program has been detected in CTCs (11). By analyzing mRNA levels of ECM network genes and Hsp47 in CTCs and primary tumor cells (26), we found that expression levels of Hsp47 and collagen genes, such as COL1A1, COL1A2, and COL4A1, were up-regulated in CTCs (Fig. 2 *A* and *B*). We asked whether Hsp47 expression contributes to cancer cell colonization and metastasis. Control and Hsp47-silenced MDA-MB-231/luc cells (*SI Appendix*, Fig. S2 *A* and *B*) were injected via tail vein into female mice with severe combined immunodeficiency (SCID). In vivo imaging system (IVIS) analysis and hematoxylin and eosin (H&E) staining results showed that Hsp47 expression was required for breast cancer cell colonization in the lung and other organs (Fig. 2 *C–E* and *SI Appendix*, Fig. S2*C*). Using the 4T1 orthotopic mammary tumor model, we confirmed that silencing Hsp47 significantly suppressed breast cancer metastasis (Fig. 2 *F* and *G* and *SI Appendix*, Fig. S2*D*).

To understand how the EMT and Hsp47 expression contribute to CTC colonization, we injected control, Twist-expressing, and Hsp47-expressing MCF10A/green fluorescent (GFP) cells in tail veins and analyzed retention of the GFP-positive cells in lungs at 4 h after injection. We found that Twist-induced EMT significantly enhanced MCF10A cell adhesion in lungs (Fig. 2 *H* and *I*). Expression of Hsp47 also promoted adhesion of MCF10A cells in lungs shortly after tail vein injection (Fig. 2 *J* and *K*). In contrast, silence of Hsp47 in 4T1 cells (4 h after tail vein injection) or MDA-MB-231 cells (4 h and 24 h after tail vein injection) significantly reduced lung retention of cancer cells (Fig. 2 *L* and *M*). These results suggest that Hsp47-induced mesenchymal phenotypes are crucial for initiation of CTC colonization.

Cancer Cell–Platelet Interaction Is Required for Hsp47-Dependent Lung Colonization. Cancer cells in circulation directly interact with platelets, red blood cells, and immune cells. Accumulated evidence suggests that platelet–cancer cell interaction plays an important role in cancer metastasis (27). We wondered whether platelets are involved in Hsp47-induced cancer cell lung colonization. Lung tissue sections from the short-term tail vein injection experiments were stained with antibody against CD41, a cell surface marker for platelets. An increased accumulation of platelets was detected around Hsp47-high MECs (Hsp47-expressing MCF10A cells or MDA-MB-231 control cells) compared with Hsp47-low MECs (control MCF10A cells or shHsp47 MDA-MB-231 cells) (Fig. 3 *A* and *B*). To perform the in vitro cancer cell–platelet binding assay, we isolated platelets from mouse blood and showed that isolated platelets were resting (*SI Appendix*, Fig. S3*A*). We found that Twist-induced EMT enhanced platelet recruitment in MCF10A cells (Fig. 3*C* and *SI Appendix*, Fig. S3*B*). HMLE clones with activated the EMT program and high Hsp47 expression were also more active in recruiting platelets compared with control clones (*SI Appendix*, Fig. S3 *C–E*). Importantly, introducing exogenous Hsp47 in MCF10A induced platelet recruitment (Fig. 3*C* and *SI Appendix*, Fig. S3*B*), while silencing Hsp47 in MDA-MB-231 cells significantly inhibited cancer cell–platelet interaction (Fig. 3 *D* and *E*).

To further determine the function of platelet recruitment in Hsp47-induced cancer cell colonization, we depleted platelet in mice using anti-GPIb antibody (*SI Appendix*, Fig. S3*F*) (28). Platelet depletion almost completely abolished Hsp47-induced lung retention of MCF10A cells (Fig. 3 *F* and *G*). Although MCF10A cells are nonmalignant and cannot form metastases in lungs, these results show that Hsp47-induced platelet recruitment is crucial for MEC adhesion or retention in the lung, the first step in cancer cell lung colonization. In addition, silencing Hsp47 failed to reduce initiation of colonization of MDA-MB-231 cells in platelet-depleted mice (Fig. 3 *H* and *I*). Therefore, EMT-associated Hsp47 expression induces cancer cell–platelet interaction, which is crucial for the initiation of cancer cell colonization.

Type I Collagen Mediates Hsp47-Dependent Platelet Recruitment and Cancer Cell Colonization. Next, we explored the molecular mechanism by which Hsp47 induces platelet recruitment and lung colonization. Type I and IV collagens are the most abundant fibrillar

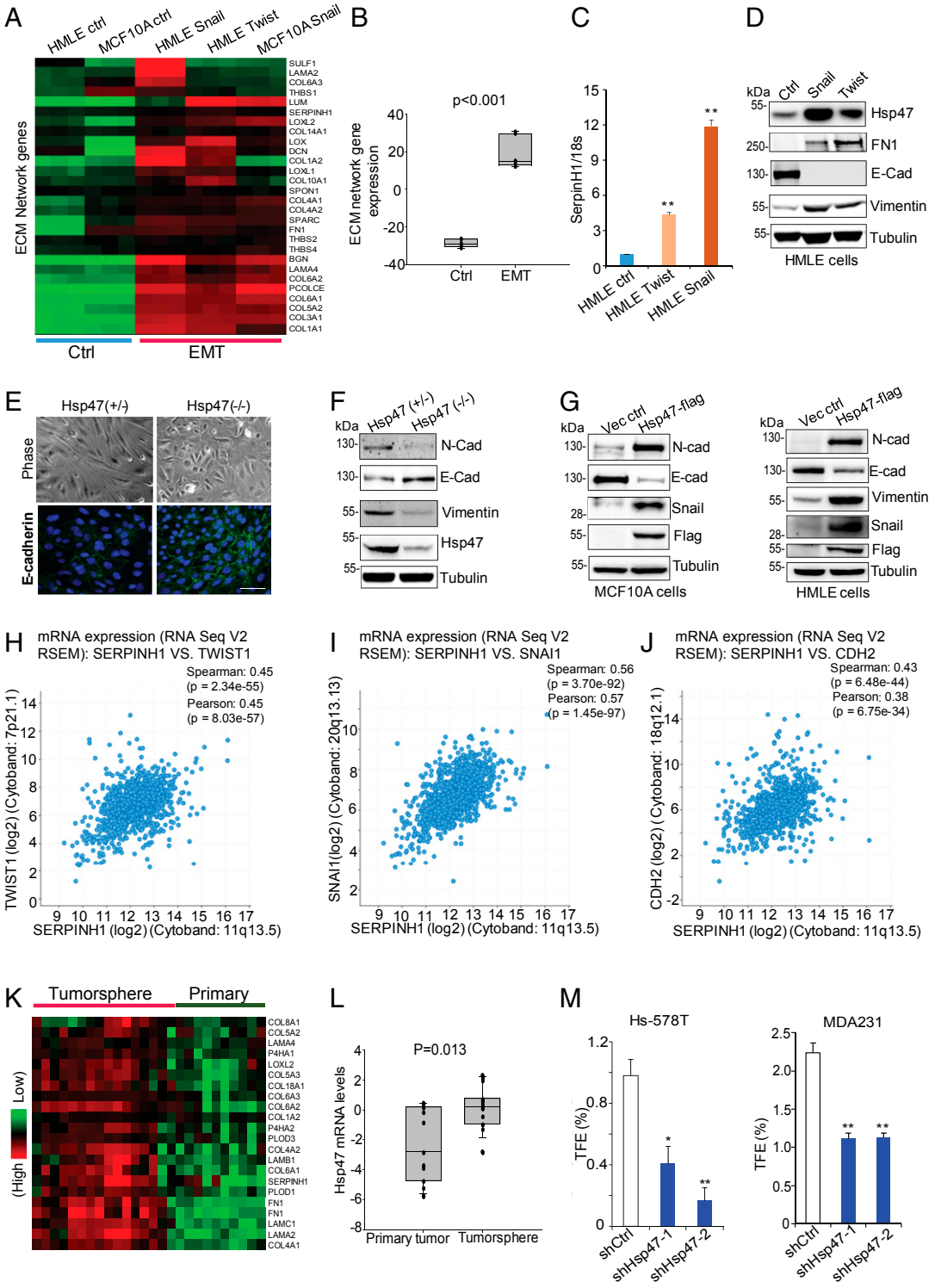

Fig. 1. Hsp47 expression induces the EMT and enhances cancer cell stemness. (*A* and *B*) Heatmap and box plot showing ECM network gene levels in control cells (MCF10 and HMLE) and cells undergoing the EMT (MCF10A-Snail, HMLE-Twist, and HMLE-Snail). The data were log2-transformed and mean-centered. Control, $n = 6$; EMT, $n = 9$; rank-sum test. (*C*) Real-time PCR data showing SerpinH1 levels in HMLE control cells and EMT cells (HMLE-Twist and HMLE-Snail). Results are presented as mean ± SEM. $n = 4$. $^{**}P < 0.01$, independent Student's t test. (*D*) Western blot analyses of Hsp47, FN, and E-Cad expression in control, Twist-expressing, and Snail-expressing HMLE cells. (*E*) Phase images and IF staining images (E-cadherin, green; nuclei, blue) of primary MECs from MMTV-Cre:Hsp47$^{+/lox}$ and MMTV-Cre:Hsp47$^{lox/lox}$ mice cultured in 2D for 5 d. (Scale bar: 25 μm.) (*F*) Western blot analyses of Hsp47 and EMT markers (N-cadherin, E-cadherin, vimentin) expression in primary MECs from MMTV-Cre:Hsp47$^{+/lox}$ and MMTV-Cre:Hsp47$^{lox/lox}$ mice cultured for 5 d. (*G*) Western blot analyses of expression of Hsp47 and EMT markers (N-cadherin, E-cadherin, vimentin, Snail) in Hsp47-expressing MCF10A cells/HMLE cells. (*H–J*) Coexpression of Hsp47 (SERPINH1) with EMT regulators TWIST1, SNAI1, and EMT marker CDH2 assessed by Spearman correlation analysis in human breast cancer tissue samples (TCGA, provisional; $n = 960$). (*K* and *L*) Heatmap and boxplot showing ECM network gene expression in tumorspheres and matched primary tumors (GSE7515). The gene expression values were derived from a published microarray dataset. The data were log2-transformed and mean-centered. Primary tumor, $n = 11$; tumorsphere, $n = 15$. (*M*) Quantification of tumorsphere formation efficiency in control and Hsp47-silenced Hs578T cells and MDA-MB-231 cells. $n = 3$. Results are presented as mean ± SEM; $^{*}P < 0.05$; $^{**}P < 0.01$, independent Student's t test.

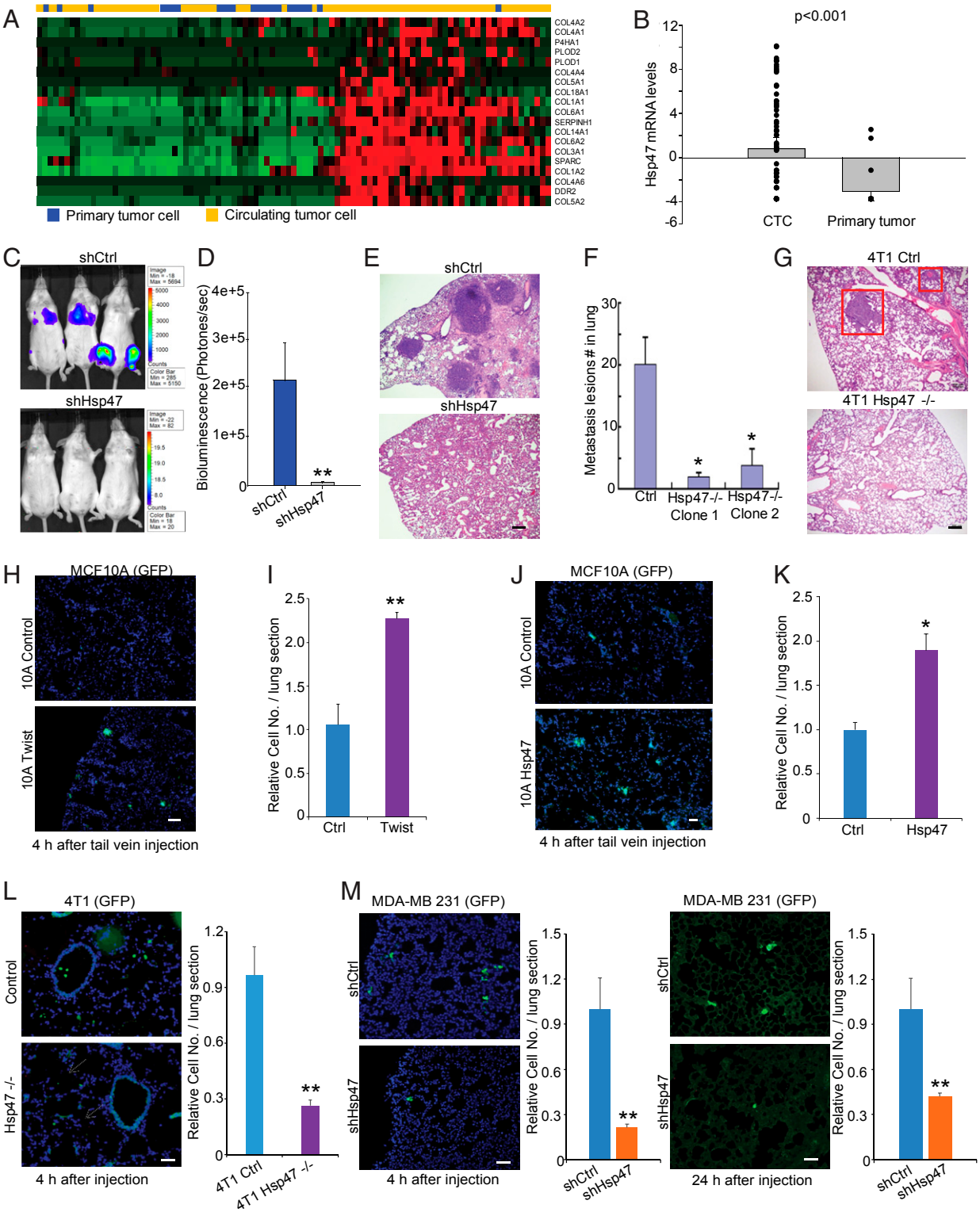

Fig. 2. Hsp47 is required for cancer cell lung colonization and metastasis. (*A*) Heatmap showing expression of ECM network genes in primary cancer cells and CTCs (GSE51372). (*B*) Boxplot showing Hsp47 mRNA levels in primary cancer cells and CTCs. CTCs, $n = 75$; primary tumor, $n = 20$. (*C*–*E*) IVIS, H&E images, and quantification showing colonization of MDA-MB-231 cells in lungs at 4 wk after injection. Mice were injected with 1×10^6 control and Hsp47-silenced MDA-MB-231/luc cells from tail vein. (Scale bar: 100 μm.) $n = 5$; independent Student's *t* test. (*F* and *G*) Lung metastasis lesions (2 wk after primary tumor removal) of control and Hsp47-silenced 4T1 cells were assessed by H&E staining in the orthotopic mammary tumor model. (Scale bar: 100 μm.) (*H* and *I*) Fluorescence microscopy images and quantification of control and Twist-expressing MCF10A/GFP cell adhesion in the lung. Lungs were collected at 4 h after tail vein injection. (Scale bar: 40 μm). $n = 3$; independent Student's *t* test. (*J* and *K*) Images and quantification of control and Hsp47-expressing MCF10A/GFP cell retention in the lung. (Scale bar: 40 μm.) $n = 3$; independent Student's *t* test. (*L* and *M*) Images and quantification of control and Hsp47-silenced 4T1/GFP cell or MDA-MB-231/GFP cell colonization in the lung. The lungs were collected at 4 h or 24 h after tail vein injection. (Scale bar: 40 μm.) $n = 3$ in *L*, $n = 5$ in *M*. Results are presented as mean ± SEM. $^{**}P < 0.01$; $^{*}P < 0.05$, independent Student's *t* test.

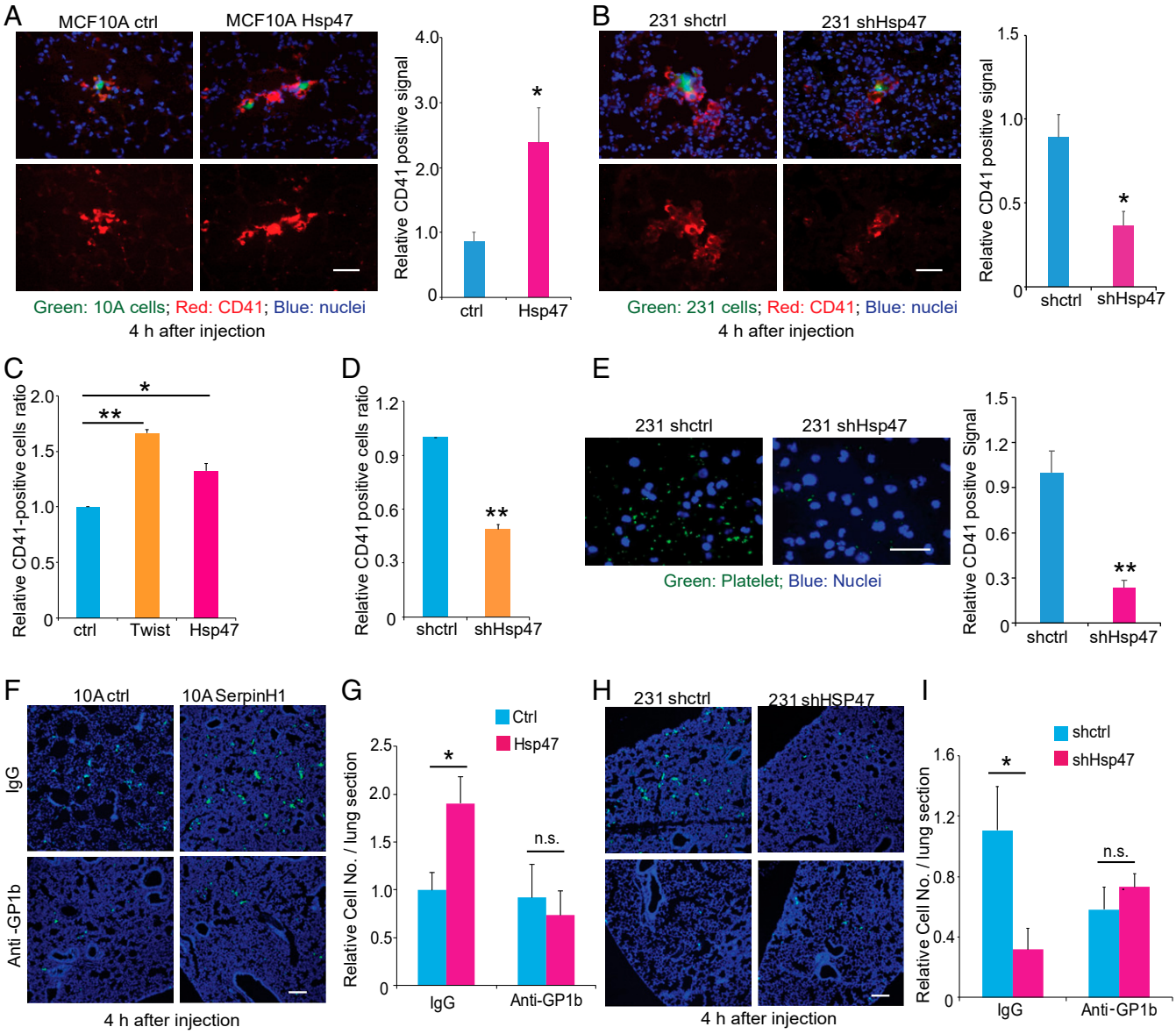

Fig. 3. Hsp47 enhances cancer cell–platelet interaction. (*A*) IF images (platelets, red; MCF10A, green; nuclei, blue) and quantification data showing the recruitment of platelets by control and Hsp47-expressing MCF10A/GFP cells in lung at 4 h after tail vein injection. (Scale bar: 40 μm.) $n = 3$; independent Student's *t* test. (*B*) IF images (platelets, red; MDA-MB-231, green; nuclei, blue) and quantification data showing the recruitment of platelets by control and Hsp47-silenced MDA-MB-231/GFP cells in the lung at 4 h after tail vein injection. (Scale bar: 40 μm.) $n = 3$; independent Student's *t* test. (*C*) FACS analysis of mouse platelet binding in control, MCF10A-Twist, and Hsp47-expressing MCF10A cells; $n = 5$; independent Student's *t* test. (*D*) FACS analysis of mouse platelet binding in control and shHsp47 MDA-MB-231 cells; $n = 4$; independent Student's *t* test. (*E*) IF images (platelets, green; DAPI, blue) and quantification data of mouse platelet binding in control and shHsp47 MDA-MB-231 cells cultured on plastic. (Scale bar: 25 μm.) $n = 3$; independent Student's *t* test. (*F* and *G*) IF images (MECs, green; DAPI, blue) and quantification of control and Hsp47-expressing MCF10A/GFP cell adhesion in the lung from mice pretreated with IgG/anti-GP1b antibody. Mice were injected with 1×10^6 MCF10A/GFP cells in the tail vein, and lungs were collected at 4 h after injection. (Scale bar: 80 μm.) $n = 4$; independent Student's *t* test. (*H* and *I*) IF images (MECs, green; DAPI, blue) and quantification of control and shHsp47 MDA-MB-231 cell retention in the lung. Mice were pretreated with IgG/anti-GP1b antibody 4 h before MDA-MB-231 cell injection. Mice were injected with 1×10^6 MDA-MB-231/GFP cells in the tail vein and lungs were collected at 4 h after injection. (Scale bar: 80 μm.) $n = 3$. Results are presented as mean ± SEM. $^{**}P < 0.01$; $^{*}P < 0.05$; n.s., not significant, independent Student's *t* test.

and basement membrane collagens, both of which were induced during the EMT and highly expressed in CTCs (Figs. 1*A* and 2*A*). Immunofluorescence images showed increased deposition of type I and IV collagen on the surface of Hsp47-expressing MCF10A spheroids (Fig. 4*A*), while silencing Hsp47 reduced type I and IV collagen deposition in MDA-MB-231 cells (Fig. 4*B*). Soluble collagen I and collagen IV were also increased in conditioned medium from Hsp47-expressing MCF10A cells compared with that from control cells (Fig. 4*C*).

To determine whether these two types of collagen mediate Hsp47 function in regulating platelet recruitment, we performed a series of in vitro and in vivo rescue experiments. Hsp47-silenced MDA231 cells were coated with type I or type IV collagen, then incubated with purified platelets. Interestingly, only type I collagen rescued cancer cell–platelet interaction in Hsp47-silenced cells (Fig. 4 *D* and *E* and *SI Appendix*, Fig. S4). Therefore, fibrillar collagen produced by cancer cells may be more potent in inducing platelet recruitment. Integrin α2β1 and glycoprotein VI (GPVI)

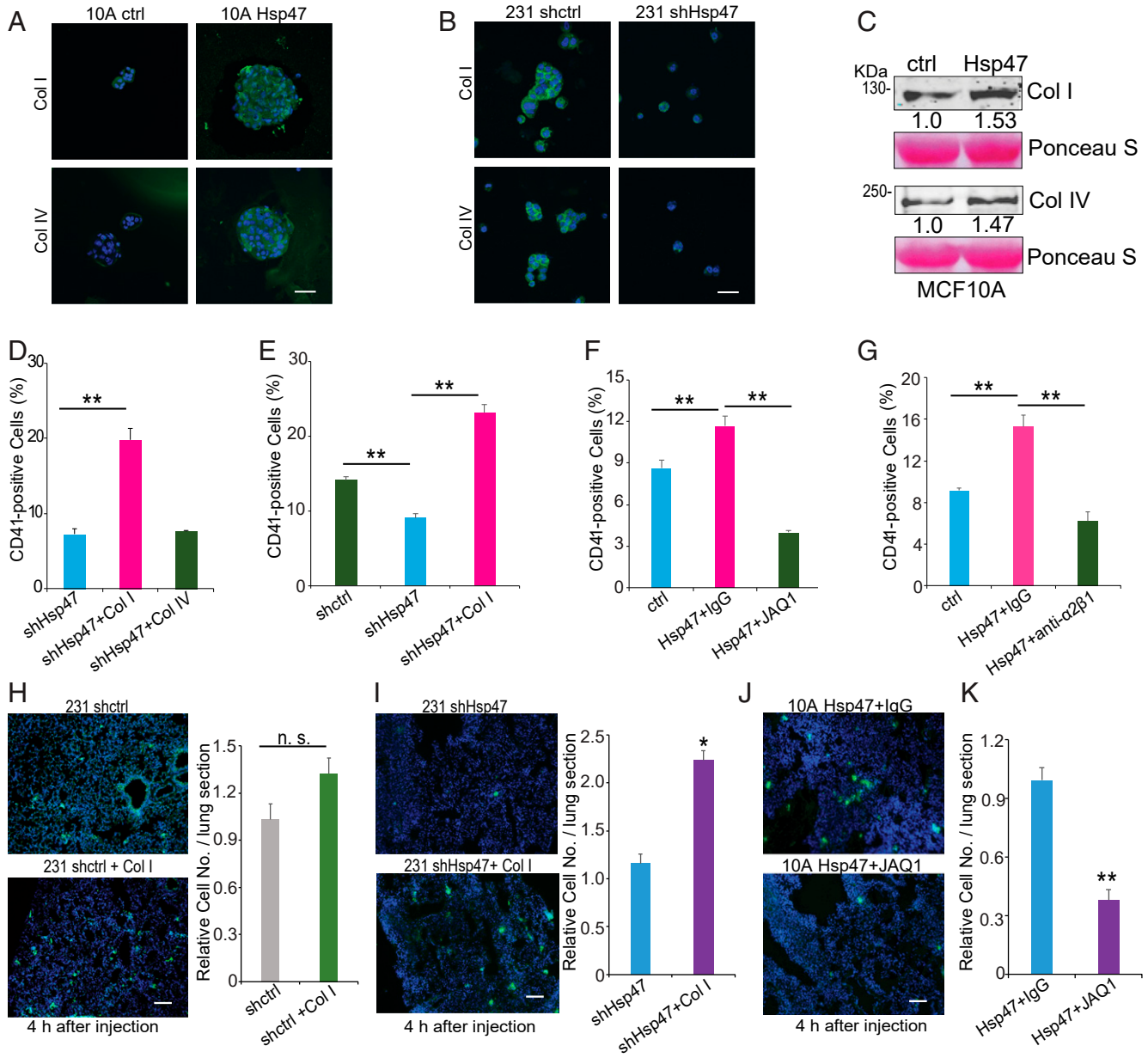

Fig. 4. Type I collagen mediates Hsp47-induced platelet recruitment. (*A*) IF images (collagen I/collagen IV, green; nuclei, blue) of control and Hsp47-expressing MCF10A cells cultured in suspension. (Scale bar: 50 μm.) (*B*) IF images (collagen I/collagen IV, green; nuclei, blue) of control and Hsp47-silenced MDA-MB-231 cells cultured in suspension. (Scale bar: 50 μm.) (*C*) Western blot analyses of collagen I and collagen IV protein levels in conditioned media derived from control and Hsp47-expressing MCF10A cells. (*D*) FACS analysis of mouse platelet binding in Hsp47-silenced MDA-MB-231 cells pretreated with collagen I or collagen IV. $n = 3$; one-way ANOVA. (*E*) FACS analysis of human platelet recruitment in control and Hsp47-silenced MDA-MB-231 cells pretreated with collagen I. $n = 3$; one-way ANOVA. (*F*) FACS analysis of platelet binding in control and Hsp47-expressing MCF10A cells incubated with IgG/JAQ1 antibody-pretreated platelets. $n = 3$; one-way ANOVA. (*G*) FACS analysis of platelet recruitment in control and Hsp47-expressing MCF10A cells. Human platelets were pretreated with IgG/integrin α2β1 blocking antibody. $n = 3$; one-way ANOVA. (*H* and *I*) IF images and quantification of vector control or Hsp47-silenced MDA-MB-231/GFP cell adhesion in lung. The cells were pretreated with/without collagen I. (Scale bar: 100 μm.) $n = 5$; independent Student's *t* test. (*J* and *K*) IF images and quantification of Hsp47-expressing MCF10A/GFP cell adhesion in lung. The mice were pretreated with IgG or JAQ1 antibody. (Scale bar: 100 μm.) $n = 5$; independent Student's *t* test. Results are presented as mean ± SEM. n.s., not significant; $^{**}P < 0.01$; $^{*}P < 0.05$.

have been identified as collagen receptors in platelets (29, 30), and collagen-platelet interaction can be inhibited with integrin α2β1- or GPVI-blocking antibodies (JAQ1) (31, 32). We found that incubation of platelets with these two blocking antibodies abolished Hsp47-induced platelet recruitment in MCF10A cells (Fig. 4 *F* and *G*).

To determine in vivo function of collagen deposition in cancer cell colonization, control and Hsp47-silenced MDA-MB-231/GFP cells were coated with type I collagen before tail vein injection. We found that treatment with collagen at least partially rescued Hsp47-silenced cancer cell retention in the lung (Fig. 4 *H* and *I*) but only slightly increased lung retention of control MDA-MB-231 cells. In another experiment, mice were treated with JAQ1 antibody before injection of Hsp47-expressing MCF10A/GFP cells. Treatment with JAQ1 antibody significantly reduced Hsp47-induced MCF10A cell adhesion in the lung (Fig. 4 *J* and *K*). These results suggest that Hsp47-dependent collagen deposition by cancer cells is crucial for the initiation of cancer cell colonization.

Hsp47-Dependent Platelet Recruitment Enhances Cancer Cell Clustering and Extravasation. Cancer cells in circulation have been detected as single cells or CTC clusters, and CTC clustering promotes cancer colonization and metastasis (33–35). Based on our observation that incubation with platelets induced cancer cell clustering in the platelet-binding experiment, we asked whether the Hsp47/collagen axis and its dependent platelet recruitment contribute to cancer cell clustering. Silencing Hsp47 in MDA-MB-231 cells moderately reduced cancer cell clustering in the absence of platelets in vitro (Fig. 5 *A* and *B*). Surprisingly, platelet incubation significantly enhanced cancer cell clustering in control MDA-MB-231 cells but only slightly increased clustering in the Hsp47-silenced cells (Fig. 5 *A* and *B*). We also found that preincubating Hsp47-silenced cells with type I collagen at least partially recovered platelet-induced clustering (Fig. 5*C* and *SI Appendix*, Fig. S5*A*). Importantly, by analyzing RNA-seq data generated from CTC samples isolated from breast cancer patients (34), we found that higher expression levels of Hsp47 and COL1A1 in CTC clusters compared with single CTCs (Fig. 5 *D* and *E*). Therefore, Hsp47/collagen axis-induced platelet recruitment may contribute to CTC clustering or to maintenance of CTC cluster integrity in vivo.

Extravasation is a necessary step for CTCs to initiate colonization. Platelet binding and activation enhance cancer cell extravasation and formation of the premetastatic niche (36). We performed transendothelial migration assay with human lung microvasculature endothelial cell (HMVEC-L) and human umbilical vein cell (HUVEC) monolayers (*SI Appendix*, Fig. S5*B*). We showed that expression of Hsp47 in MCF10A cells increased platelet-induced transendothelial migration (Fig. 5 *F–H*), and this increase was blocked by the JAQ1 antibody (Fig. 5 *G* and *H* and *SI Appendix*, Fig. S5*C*) or integrin α2β1 antibody (*SI Appendix*, Fig. S5 *D* and *E*). In addition, transendothelial migration of control MDA-MB-231 cells, but not of Hsp47-silenced cells, was significantly enhanced after incubation with platelets (Fig. 5*I*). Pretreatment with type I collagen rescued transendothelial migration in Hsp47-silenced MDA231 cells (Fig. 5 *J* and *K* and *SI Appendix*, Fig. S5 *F* and *G*). These data suggest that activation of the Hsp47/collagen axis promotes cancer cell extravasation by inducing platelet recruitment.

Hsp47 Expression and Gene Amplification in Human Breast Cancer Tissues. The Hsp47 gene (SERPINH1) locates at a region often amplified in cancer. Amplification of the Hsp47 gene was identified in 6% human breast cancer tissues and in 11% metastatic breast cancer tissues (Fig. 6 *A* and *B*). Importantly, increased Hsp47 expression in tumor tissue correlated with short distant recurrent-free survival in breast cancer patients (Fig. 6*C* and *SI Appendix*, Fig. S6*A*). These results indicate that gene amplification and increased expression of Hsp47 are associated with cancer metastasis.

Activation of the EMT program has been detected in basal-like cells and TNBC cells (37). TNBC cells are also associated with a high incidence of cancer metastasis and poor prognosis (38). Using immunohistochemistry (IHC) analysis of a human breast cancer tissue array containing 217 samples, we showed that Hsp47 protein levels were significantly higher in TNBC cells compared with other subtypes (Fig. 6 *D* and *E*). Consistent with data from human breast cancer tissue, our previous study found higher Hsp47 mRNA levels in basal-like breast cancer cell lines compared with the luminal subtype (20). In the present study, we found increased Hsp47 protein expression in basal cancer cell lines compared with luminal cancer cell lines (Fig. 6 *F* and *G*); increased secretion and deposition of type I collagen have also been detected in basal cancer cell lines (39).

We showed that Hsp47 expression is crucial for the initiation of cancer cell colonization. To further elucidate the role of Hsp47 in the late stage of cancer cell colonization, we introduced an inducible Hsp47 silencing system in MDA-MB-231 cells. Hsp47 expression was knocked down from 24 h or 7 d after tail vein injection (*SI Appendix*, Fig. S6*B*). We found that silencing Hsp47 at the late stage of cancer cell colonization also inhibited tumor lesion formation in lungs (Fig. 6 *H–J*). These results suggest that increased Hsp47 expression in cancer cells contributes to both the initiation of cancer cell colonization and the formation of macrometastases.

Discussion

Clinical evidence and data from mouse tumor models strongly support the "seed and soil" hypothesis that cancer metastasis requires favorable interactions between metastatic tumor cells (the "seed") and the tissue microenvironment (the "soil") (40). Recent advances in TICs and CTCs have provided additional insight into the "seed" metastatic cancer cells (41, 42). Here we show that CTCs and the TIC-enriched cell population exhibit increased expression of chaperone protein Hsp47 and its target collagen. Increased expression of Hsp47 and Hsp47-dependent collagen deposition are crucial for cancer cell–platelet interaction and platelet-dependent cancer cell colonization in the lung (Fig. 6*K*). These results suggest that metastatic cancer cells can produce and carry the "soil" (i.e., collagen) when traveling from primary tumors to distal sites, and that the self-deposited collagen is crucial for cancer cell colonization at distant organs.

EMT and mesenchymal-epithelial transition dynamics play a critical role in cancer metastasis. The EMT induces cancer cell invasion and contributes to cancer metastasis at an early stage (7). Expression of Hsp47 mRNA is induced during the EMT and is associated with EMT markers in human breast cancer tissues, suggesting that Hsp47 expression is regulated at the transcription level. Nevertheless, we cannot rule out the possibility that Hsp47 is also regulated at the protein level (translation or protein stability) during the EMT. We previously showed that miR-29 is a negative regulator of Hsp47 (20). Down-regulation of miR-29 may contribute to Hsp47 induction during the EMT. Deletion of Hsp47 in MECs inhibited the EMT and suppressed the mesenchymal phenotypes, including collagen deposition, cell migration, and invasion. The EMT is relevant to the acquisition and maintenance of stem cell-like characteristics and is sufficient to endow differentiated normal and cancer cells with stem cell properties (43, 44).

The function of collagen signaling in the EMT is well characterized. Type I collagen and its receptor discoidin domain-containing receptor 2 (DDR2) can promote the EMT by enhancing Snail stability (45). Increased collagen expression or deposition is associated with poor prognosis in breast cancer patients (46, 47). Inhibition of collagen production and cross-linking represses cancer progression and metastasis (48, 49). Interestingly, exogenous type I collagen can only partially rescue EMT phenotypes in Hsp47-silenced cells. We recently identified DDR2 as a target of Hsp47 (50). DDR2 may also contribute to Hsp47-induced mesenchymal phenotypes.

Single-cell sequencing data have shown increased expression of the EMT and stemness markers in CTCs (12). It has been postulated that activation of the EMT program facilitates CTC generation and enhances cancer cell survival in the circulation system (7, 51). We found that Twist-induced EMT significantly enhanced MEC–platelet interaction, platelet-dependent extravasation, and MEC retention in the lung. Platelets are originally derived from megakaryocytes in the bone marrow (52), and one of their functions is to prevent bleeding and reduce blood loss in the event of vascular injury (53). Platelet count is associated with metastasis and poor prognosis in cancer patients (54, 55). The long-term use of low-dose antiplatelet drugs, such as aspirin, inhibits cancer metastasis and significantly reduces cancer incidence (56, 57). Our data show that Hsp47-induced mesenchymal phenotypes enhance CTC colonization by inducing cancer cell–platelet interaction. It has been reported that incubation of platelets with cancer cells induces the release of TGF-β, which subsequently activates the TGF-β/Smad and nuclear factor kappa-light-chain-enhancer of activated B cells pathways in cancer cells and promotes their transition to an invasive mesenchymal-like

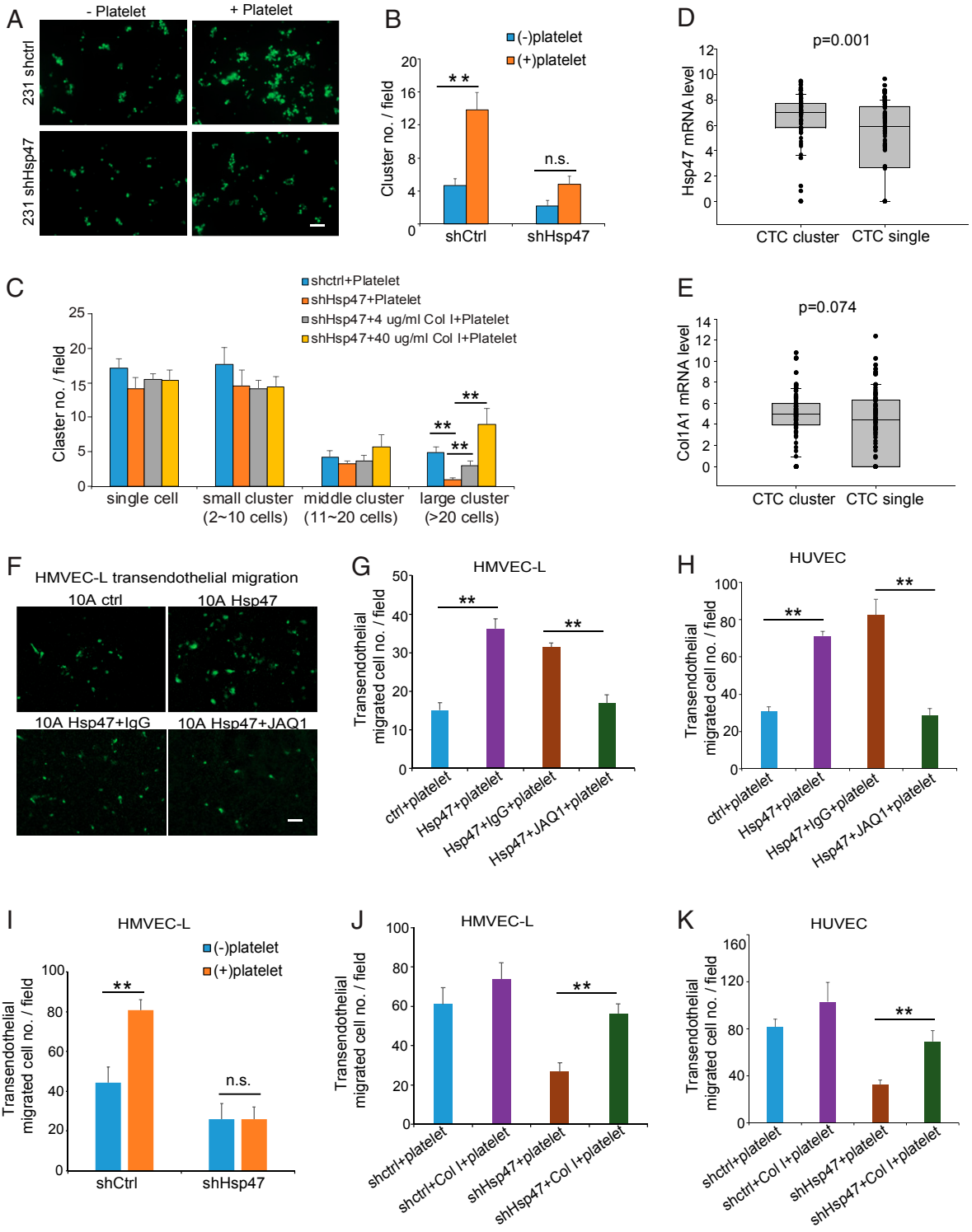

Fig. 5. Hsp47-dependent platelet recruitment enhanced cancer cell clustering and extravasation. (*A* and *B*) Images and quantification of cells clustering in control or Hsp47-silenced MDA-MB-231/GFP cells in the presence or absence of mouse platelets. (Scale bar: 100 μm.) $n = 6$, independent Student's t test. (*C*) Quantification of cell clustering in control or Hsp47-silenced MDA-MB-231/GFP cells in the presence or absence of mouse platelets. Cells were treated with collagen I (0, 4, or 40 μg/mL) before platelet incubation. $n = 6$; one-way ANOVA. (*D* and *E*) Quantification of Hsp47 and ColA1 mRNA levels in single CTCs and CTC clusters based on the RNA-seq data generated from breast cancer patient CTC samples. $n = 78$ (CTC cluster) and 94 (single CTC) (GSE111065). (*F* and *G*) Images and quantification of MCF10A extravasation in the HMVEC-L transendothelial migration assay. Control or Hsp47-expressing MCF10A/GFP cells were incubated with IgG/JAQ1 antibody- treated platelets before the assay. (Scale bar: 100 μm.) $n = 3$; one-way ANOVA. (*H*) Quantification of MCF10A extravasation in the HUVEC transendothelial migration assay. Control or Hsp47-expressing MCF10A/GFP cells were incubated with IgG/JAQ1 antibody-treated platelets before the assay. (Scale bar: 100 μm.) $n = 5$; one-way ANOVA. (*I*) Quantification of MDA-MB-231 cell extravasation in the HMVEC-L transendothelial migration assay. Control or Hsp47-silenced MDA-MB-231/GFP cells were incubated with or without mouse platelets before being plated in transendothelial assay chambers. (Scale bar: 100 μm.) $n = 8$; independent Student's t test. (*J* and *K*) Quantification of cancer cell extravasation in HMVEC-L and HUVEC transendothelial migration assay. Control or Hsp47-silenced MDA-MB-231/GFP cells were treated with collagen I (0 or 4 μg/mL) before platelet incubation. $n = 3$. Results are presented as mean ± SEM. $^{**}P < 0.01$; $^{*}P < 0.05$; n.s., not significant, one-way ANOVA.

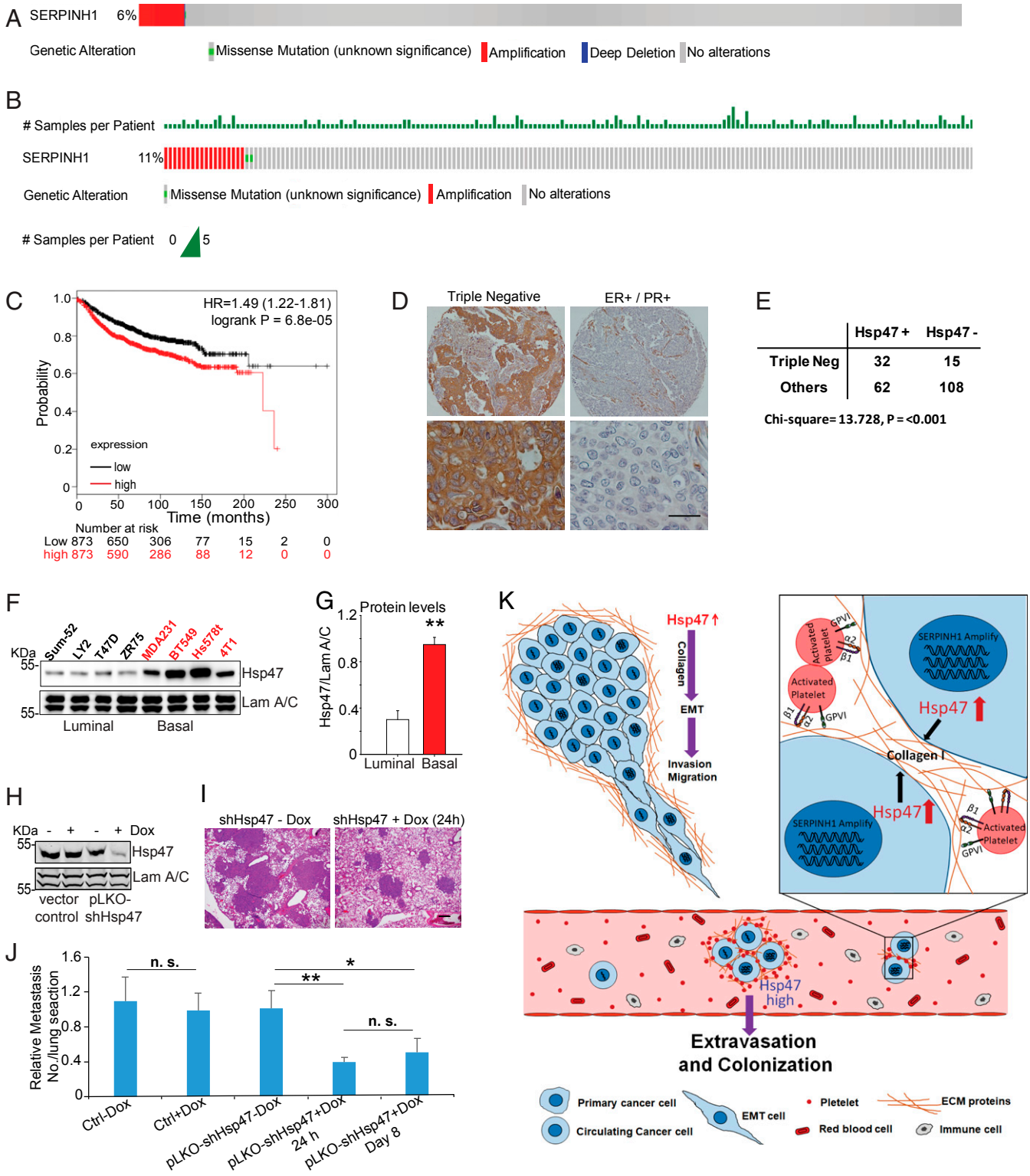

Fig. 6. Hsp47 gene amplification and expression are associated with human breast cancer metastasis. (*A* and *B*) Hsp47 gene (SERPINH1) amplification in invasive breast carcinoma (n = 963) and metastatic breast cancer (n = 237). Data were from TCGA and the Metastatic Breast Cancer Project (provisional, October 2018). (*C*) Kaplan–Meier analysis showing the association of Hsp47 expression with distant recurrence-free survival in breast cancer patients. n = 1,746. (*D*) IHC images showing Hsp47 expression in ER-positive and TNBC tissues. (Scale bar: 25 μm.) (*E*) Quantification of Hsp47 staining from *D*; the data were analyzed by the χ^2 test. (*F* and *G*) Hsp47 protein levels were assessed and quantified in a panel of breast cancer cell lines. n = 4; independent Student's t test. Results are presented as mean ± SEM. $^{**}P < 0.01$. (*H*) Western blot analysis of Hsp47 levels in control and pLKO-shHsp47 MDA-MB 231 cells after doxycycline treatment (200 ng/mL). (*I* and *J*) H&E images and quantification data showing the lung colonization of MDA-MB-231 cells at 5 wk after tail vein injection. 1×10^6 control and pLKO-shHsp47 MDA-MB-231 cells were injected in the tail vein, and doxycycline treatment was started on day 1 or 7 postinjection. (Scale bar: 100 μm.) Vector control group, n = 8; pLKO-shHsp47 group, n = 18. Results are presented as mean ± SEM. $^{**}P < 0.01$; $^{*}P < 0.05$; n.s., not significant, one-way ANOVA. (*K*) Scheme showing how the Hsp47/collagen axis promotes the EMT and cancer metastasis.

phenotype (58). Therefore, a positive feedback loop may exist between cancer cell–platelet interaction and EMT induction.

Expression levels of Hsp47 and ECM network genes are upregulated in CTCs compared with primary tumors. Hsp47 expression in MECs induced platelet recruitment, which is crucial for the initiation of lung colonization of cancer cells. Secretion/deposition of collagen I and IV are both regulated by Hsp47 in breast cancer cells (20); interestingly, we found that cancer cell–platelet interaction is mediated mainly by type I collagen. During vascular injury, platelets directly interact with subendothelial collagen, triggering the formation of a hemostatic plug (59). Using the platelet-specific deletion mouse model, a recent study shows that Hsp47 on platelet surface enhances GPVI-collagen binding and platelet activation (60). It is not clear whether platelet-derived Hsp47 contributes to cancer cell–platelet interaction. Tissue factor (TF), an initiator of the extrinsic coagulation cascade, is expressed in breast cancer tissue and plays important roles in cancer progression and metastasis (61). However, induction of TF expression has not been detected during the EMT and in CTCs, and TF is unlikely to serve as the downstream target of Hsp47 to promote the EMT-related cancer cell–platelet interaction.

It has been reported that only small number of CTCs can survive and colonize in the secondary organs; the majority of cancer cells die after tail vein injection (62). Platelet binding and activation enhances cancer cell survival in the circulation and facilitates extravasation and formation of a premetastatic niche (4). We found that silencing Hsp47 expression significantly reduced cancer cell numbers in lung after 24 h, suggesting that Hsp47-induced platelet recruitment contributes to extravasation and initial colonization of cancer cells. In coculture experiments, we showed that Hsp47-induced platelet recruitment enhanced the extravasation of MECs. ATP has been identified as a key mediator of platelet-induced extravasation (36). A recent study showed that the COX-1/TXA2 pathway in platelets is required for the aggregation of platelets on cancer cells and formation of the premetastatic niche (63). Platelet activation also induces the release of platelet-derived factors, including TGF-β, vascular endothelial growth factor, and platelet-derived growth factor. The functions of these growth factors in cancer invasion, angiogenesis, and metastasis have been well characterized. It is important to determine whether the Hsp47/collagen axis induces these pathways and the release of platelet-derived factors, and subsequently promotes formation of the premetastatic niche.

Cancer cells in circulation have been detected as single CTCs or CTC clusters containing 2 to 50 cells (33). Studies in mouse models indicate that CTC clusters have 20- to 50-fold greater metastatic potential (33). Clinical evidence also suggests a link between CTC clusters and worse clinical outcomes (64, 65). Plakoglobin, a cell–cell junction protein highly expressed in CTC clusters, contributes to cluster formation and integrity in the blood (33). Interestingly, we found that expression of Hsp47 was significantly higher in CTC clusters compared with single CTC cells in clinical samples. Hsp47/collagen-induced platelet recruitment enhanced cancer cell clustering in vitro. It has been proposed that CTC clusters are derived from primary tumors or from the aggregation/proliferation of single CTCs; however, current evidence does not support the concept that CTC clusters form by aggregation of single CTCs (33). Platelets and platelet-derived microparticles are detected in primary tumors (66); therefore, Hsp47/collagen-induced platelet recruitment may facilitate cancer cell clustering in the primary tumor or maintain the integrity of CTC clusters in circulation. Cancer cells and CAFs both produce significant amounts of collagen and other ECM proteins in primary tumor tissue, and CAF-derived collagen may also contribute to platelet recruitment and activation in primary tumor tissue.

Our study provides insight into how mesenchymal phenotypes in CTCs induce platelet recruitment and enhance cancer cell colonization. We have identified the Hsp47/collagen axis as a critical regulator of the cancer cell–platelet interaction. Collagen is not an ideal druggable target; however, small-molecule compounds that inhibit Hsp47–collagen interaction have been characterized recently (67). Therefore, targeting the Hsp47/collagen axis is a potential strategy to inhibit cancer cell colonization and metastasis.

Materials and Methods

Fluorescence-Activated Cell Sorting of Platelet Recruitment. To analyze cancer cell-platelet interaction, CD41 (platelet marker) levels on tumor cells were examined by fluorescence-activated cell sorting (FACS) analysis. Mouse platelets were freshly prepared before incubation with cancer cells. Blood was collected from abdominal aortas of isofluorane-anesthetized mice using 1/7th volume of ACD (85 mM trisodium citrate, 83 mM dextrose, and 21 mM citric acid) as an anticoagulant (68). Platelets were then washed once with CGS (0.12 M sodium chloride, 0.0129 M trisodium citrate, and 0.03 M D-glucose, pH 6.5) and resuspended in 3×10^8/mL and incubated for 1 h at room temperature before use. Platelet aggregation was measured with a CHRONO-LOG Model 700 Whole Blood/Optical Lumi-Aggregometer at 37 °C with stirring (1,000 rpm). Tumor cells were trypsinized and resuspended as 1×10^6 cells in 200 μL of Tyrode's buffer (120 mM $NaHCO_3$, 138 mM NaCl, 5.5 mM glucose, 2.9 mM KCl, 2 mM $MgCl_2$, 10 mM Hepes, and 0.42 mM Na_2HPO_4, pH 7.4), then incubated with 400 μL of 3×10^8/mL mouse platelets at 37 °C for 60 min. After incubation with platelets, samples were fixed in 2% paraformaldehyde at room temperature for 20 min and then stained with CD41-fluorescein isothiocyanate (FITC) Ab (BD Biosciences; 553848) at room temperature for 40 min, protected from light. FACS analysis was done with a BD LSR II flow cytometer, and data were analyzed by CellQuest Pro (BD Biosciences). Gates were set according to unstaining control and single color controls for FITC.

Clustering Assay. Control or shHsp47 lentivirus-infected MDA-MB-231/GFP cells (1×10^5) were preincubated with or without 4 μg/mL or 40 μg/mL type I collagen for 30 min at room temperature. After incubation, cells were centrifuged at 1,000 rpm for 3 min and suspended in 300 μL of Tyrode's buffer, then incubated with or without 100 μL mouse platelets in nonadherent 24-well culture plates for 60 min at 37 °C. Images were obtained with a Nikon microscope, and the number of cell clusters was quantified.

Transendothelial Migration Assay. HUVEC or HMVEC-L (5×10^4 cells/well) were plated on the 8-μm-pore polycarbonate membrane insert (Transwell; Corning) and cultured for 2 to 3 d to confluence. MDA-MB 231/GFP cells (1×10^5 cells per well) in 300 μL of DMEM/F12 medium with 10% FBS with or without platelet/collagen I pretreatment were added on the upper chamber. An additional 500 μL of DMEM/F12 medium with 10% FBS medium was added to the lower chamber each well. Cells were incubated at 37 °C for 24 h and fixed by 100% methanol. Cells were removed from the upper chamber by gently wiping the upper surface of the membrane with a cotton swab. MDA-MB 231/GFP cells invaded through the HUVEC layer were imaged with a Nikon microscope, and invaded cells were quantified.

***In Vivo* Xenograft Experiments.** Six-week-old female SCID mice were randomly grouped and injected with 1×10^6 malignant or nonmalignant MECs via tail vein or in mammary fat pads. All procedures were performed in accordance with the guidelines of the Division of Laboratory Animal Resources at the University of Kentucky.

Patient Survival Analysis and Other Statistical Analysis. To address the clinical relevance of enhanced Hsp47 expression, we assessed the association between mRNA levels of Hsp47 and patient survival using the published microarray data generated from 1,746 human TNBC tissue samples (69). Tumor samples were split into 2 equal-sized groups of low and high Hsp47 expression based on mRNA levels. Significant differences in overall survival time were assessed using the Cox proportional hazard (log-rank) test.

All experiments were repeated at least twice. Results were reported as mean ± SEM; the significance of difference was assessed by the χ^2 test, independent Student's t test, or one-way analysis of variance (ANOVA) with SigmaPlot 12.3 (Systat Software). $P < 0.05$ represents statistical significance, and $P < 0.01$ represents sufficiently statistical significance. All reported P values are derived from two-tailed tests.

More detailed information about the materials and methods of this study are provided in *SI Appendix*.

Data Availability Statement. All data in this manuscript are freely available. The gene expression data generated from this study have been deposited in the Gene Expression Omnibus (GEO) database, https://www.ncbi.nlm.nih.gov/geo (accession no GSE143349) (70).

MEDICAL SCIENCES

ACKNOWLEDGMENTS. We appreciate the technical support provided by the University of Kentucky Flow Cytometry and Cell Sorting Core Facility; and the Biospecimen Procurement and Translational Pathology Shared Resource Facility at the Markey Cancer Center (P30CA177558). This study was supported by National Cancer Institute Grants 1R01 CA207772, 1R01 CA215095, and 1R21 CA209045 (to R.X.).

1. D. Hanahan, R. A. Weinberg, Hallmarks of cancer: The next generation. *Cell* **144**, 646–674 (2011).
2. A. W. Lambert, D. R. Pattabiraman, R. A. Weinberg, Emerging biological principles of metastasis. *Cell* **168**, 670–691 (2017).
3. D. S. Micalizzi, S. Maheswaran, D. A. Haber, A conduit to metastasis: Circulating tumor cell biology. *Genes Dev.* **31**, 1827–1840 (2017).
4. L. J. Gay, B. Felding-Habermann, Contribution of platelets to tumour metastasis. *Nat. Rev. Cancer* **11**, 123–134 (2011).
5. E. Rossi *et al*., M30 neoepitope expression in epithelial cancer: Quantification of apoptosis in circulating tumor cells by CellSearch analysis. *Clin. Cancer Res.* **16**, 5233–5243 (2010).
6. M. Giuliano *et al*., Perspective on circulating tumor cell clusters: Why it takes a village to metastasize. *Cancer Res.* **78**, 845–852 (2018).
7. J. H. Tsai, J. Yang, Epithelial-mesenchymal plasticity in carcinoma metastasis. *Genes Dev.* **27**, 2192–2206 (2013).
8. A. Puisieux, T. Brabletz, J. Caramel, Oncogenic roles of EMT-inducing transcription factors. *Nat. Cell Biol.* **16**, 488–494 (2014).
9. R. Kalluri, R. A. Weinberg, The basics of epithelial-mesenchymal transition. *J. Clin. Invest.* **119**, 1420–1428 (2009).
10. R. Chakrabarti *et al*., Elf5 inhibits the epithelial-mesenchymal transition in mammary gland development and breast cancer metastasis by transcriptionally repressing Snail2. *Nat. Cell Biol.* **14**, 1212–1222 (2012).
11. M. Yu *et al*., Circulating breast tumor cells exhibit dynamic changes in epithelial and mesenchymal composition. *Science* **339**, 580–584 (2013).
12. C. L. Chen *et al*., Single-cell analysis of circulating tumor cells identifies cumulative expression patterns of EMT-related genes in metastatic prostate cancer. *Prostate* **73**, 813–826 (2013).
13. C. Frantz, K. M. Stewart, V. M. Weaver, The extracellular matrix at a glance. *J. Cell Sci.* **123**, 4195–4200 (2010).
14. P. Lu, V. M. Weaver, Z. Werb, The extracellular matrix: A dynamic niche in cancer progression. *J. Cell Biol.* **196**, 395–406 (2012).
15. T. Oskarsson *et al*., Breast cancer cells produce tenascin C as a metastatic niche component to colonize the lungs. *Nat. Med.* **17**, 867–874 (2011).
16. C. M. Williams, A. J. Engler, R. D. Slone, L. L. Galante, J. E. Schwarzbauer, Fibronectin expression modulates mammary epithelial cell proliferation during acinar differentiation. *Cancer Res.* **68**, 3185–3192 (2008).
17. A. Naba *et al*., The matrisome: In silico definition and in vivo characterization by proteomics of normal and tumor extracellular matrices. *Mol. Cell. Proteomics* **11**, M111.014647 (2012).
18. G. Xiong, L. Deng, J. Zhu, P. G. Rychahou, R. Xu, Prolyl-4-hydroxylase α subunit 2 promotes breast cancer progression and metastasis by regulating collagen deposition. *BMC Cancer* **14**, 1 (2014).
19. J. B. Ross, D. Huh, L. B. Noble, S. F. Tavazoie, Identification of molecular determinants of primary and metastatic tumour re-initiation in breast cancer. *Nat. Cell Biol.* **17**, 651–664 (2015).
20. J. Zhu *et al*., Chaperone Hsp47 drives malignant growth and invasion by modulating an ECM gene network. *Cancer Res.* **75**, 1580–1591 (2015).
21. R. Xu, J. H. Mao, Gene transcriptional networks integrate microenvironmental signals in human breast cancer. *Integr. Biol.* **3**, 368–374 (2011).
22. Y. Ishida, K. Nagata, Hsp47 as a collagen-specific molecular chaperone. *Methods Enzymol.* **499**, 167–182 (2011).
23. X. Huang, S. M. Gollin, S. Raja, T. E. Godfrey, High-resolution mapping of the 11q13 amplicon and identification of a gene, TAOS1, that is amplified and overexpressed in oral cancer cells. *Proc. Natl. Acad. Sci. U.S.A.* **99**, 11369–11374 (2002).
24. Y. J. Kwon *et al*., Expression patterns of aurora kinase B, heat shock protein 47, and periostin in esophageal squamous cell carcinoma. *Oncol. Res.* **18**, 141–151 (2009).
25. C. J. Creighton *et al*., Residual breast cancers after conventional therapy display mesenchymal as well as tumor-initiating features. *Proc. Natl. Acad. Sci. U.S.A.* **106**, 13820–13825 (2009).
26. D. T. Ting *et al*., Single-cell RNA sequencing identifies extracellular matrix gene expression by pancreatic circulating tumor cells. *Cell Rep.* **8**, 1905–1918 (2014).
27. J. P. Stone, D. D. Wagner, P-selectin mediates adhesion of platelets to neuroblastoma and small cell lung cancer. *J. Clin. Invest.* **92**, 804–813 (1993).
28. B. Xiang *et al*., Platelets protect from septic shock by inhibiting macrophage-dependent inflammation via the cyclooxygenase 1 signalling pathway. *Nat. Commun.* **4**, 2657 (2013).
29. B. P. Nuyttens, T. Thijs, H. Deckmyn, K. Broos, Platelet adhesion to collagen. *Thromb. Res.* **127** (suppl. 2), S26–S29 (2011).
30. M. Haemmerle, R. L. Stone, D. G. Menter, V. Afshar-Kharghan, A. K. Sood, The platelet lifeline to cancer: Challenges and opportunities. *Cancer Cell* **33**, 965–983 (2018).
31. M. W. Miller *et al*., Small-molecule inhibitors of integrin alpha2beta1 that prevent pathological thrombus formation via an allosteric mechanism. *Proc. Natl. Acad. Sci. U.S.A.* **106**, 719–724 (2009).
32. B. Nieswandt *et al*., Long-term antithrombotic protection by in vivo depletion of platelet glycoprotein VI in mice. *J. Exp. Med.* **193**, 459–469 (2001).
33. N. Aceto *et al*., Circulating tumor cell clusters are oligoclonal precursors of breast cancer metastasis. *Cell* **158**, 1110–1122 (2014).
34. S. Gkountela *et al*., Circulating tumor cell clustering shapes DNA methylation to enable metastasis seeding. *Cell* **176**, 98–112.e14 (2019).
35. X. Liu *et al*., Homophilic CD44 interactions mediate tumor cell aggregation and polyclonal metastasis in patient-derived breast cancer models. *Cancer Discov.* **9**, 96–113 (2019).
36. D. Schumacher, B. Strilic, K. K. Sivaraj, N. Wettschureck, S. Offermanns, Platelet-derived nucleotides promote tumor-cell transendothelial migration and metastasis via P2Y2 receptor. *Cancer Cell* **24**, 130–137 (2013).
37. D. Sarrió *et al*., Epithelial-mesenchymal transition in breast cancer relates to the basal-like phenotype. *Cancer Res.* **68**, 989–997 (2008).
38. E. A. Rakha, I. O. Ellis, Triple-negative/basal-like breast cancer: Review. *Pathology* **41**, 40–47 (2009).
39. G. Xiong *et al*., Collagen prolyl 4-hydroxylase 1 is essential for HIF-1α stabilization and TNBC chemoresistance. *Nat. Commun.* **9**, 4456 (2018).
40. H. Peinado *et al*., Pre-metastatic niches: Organ-specific homes for metastases. *Nat. Rev. Cancer* **17**, 302–317 (2017).
41. M. Y. Kim *et al*., Tumor self-seeding by circulating cancer cells. *Cell* **139**, 1315–1326 (2009).
42. L. Zhang *et al*., The identification and characterization of breast cancer CTCs competent for brain metastasis. *Sci. Transl. Med.* **5**, 180ra48 (2013).
43. H. Y. Jung, J. Yang, Unraveling the TWIST between EMT and cancer stemness. *Cell Stem Cell* **16**, 1–2 (2015).
44. U. Wellner *et al*., The EMT-activator ZEB1 promotes tumorigenicity by repressing stemness-inhibiting microRNAs. *Nat. Cell Biol.* **11**, 1487–1495 (2009).
45. K. Zhang *et al*., The collagen receptor discoidin domain receptor 2 stabilizes SNAIL1 to facilitate breast cancer metastasis. *Nat. Cell Biol.* **15**, 677–687 (2013).
46. M. W. Conklin *et al*., Aligned collagen is a prognostic signature for survival in human breast carcinoma. *Am. J. Pathol.* **178**, 1221–1232 (2011).
47. L. J. van 't Veer *et al*., Gene expression profiling predicts clinical outcome of breast cancer. *Nature* **415**, 530–536 (2002).
48. J. T. Erler *et al*., Hypoxia-induced lysyl oxidase is a critical mediator of bone marrow cell recruitment to form the premetastatic niche. *Cancer Cell* **15**, 35–44 (2009).
49. D. M. Gilkes *et al*., Collagen prolyl hydroxylases are essential for breast cancer metastasis. *Cancer Res.* **73**, 3285–3296 (2013).
50. J. Chen, S. Wang, Z. Zhang, C. I. Richards, R. Xu, Heat shock protein 47 (HSP47) binds to discoidin domain-containing receptor 2 (DDR2) and regulates its protein stability. *J. Biol. Chem.* **294**, 16846–16854 (2019).
51. W. C. Wang *et al*., Survival mechanisms and influence factors of circulating tumor cells. *BioMed Res. Int.* **2018**, 6304701 (2018).
52. K. R. Machlus, J. N. Thon, J. E. Italiano, Jr, Interpreting the developmental dance of the megakaryocyte: A review of the cellular and molecular processes mediating platelet formation. *Br. J. Haematol.* **165**, 227–236 (2014).
53. H. H. Versteeg, J. W. Heemskerk, M. Levi, P. H. Reitsma, New fundamentals in hemostasis. *Physiol. Rev.* **93**, 327–358 (2013).
54. L. A. Tjon-Kon-Fat *et al*., Platelets harbor prostate cancer biomarkers and the ability to predict therapeutic response to abiraterone in castration resistant patients. *Prostate* **78**, 48–53 (2018).
55. M. Zhang *et al*., High platelet-to-lymphocyte ratio predicts poor prognosis and clinicopathological characteristics in patients with breast cancer: A meta-analysis. *BioMed Res. Int.* **2017**, 9503025 (2017).
56. P. Patrignani, C. Patrono, Aspirin and cancer. *J. Am. Coll. Cardiol.* **68**, 967–976 (2016).
57. P. M. Rothwell *et al*., Effect of daily aspirin on risk of cancer metastasis: A study of incident cancers during randomised controlled trials. *Lancet* **379**, 1591–1601 (2012).
58. M. Labelle, S. Begum, R. O. Hynes, Direct signaling between platelets and cancer cells induces an epithelial-mesenchymal-like transition and promotes metastasis. *Cancer Cell* **20**, 576–590 (2011).
59. R. W. Farndale, J. J. Sixma, M. J. Barnes, P. G. de Groot, The role of collagen in thrombosis and hemostasis. *J. Thromb. Haemost.* **2**, 561–573 (2004).
60. P. Sasikumar *et al*., The chaperone protein HSP47: A platelet collagen binding protein that contributes to thrombosis and hemostasis. *J. Thromb. Haemost.* **16**, 946–959 (2018).
61. T. Ueno, M. Toi, M. Koike, S. Nakamura, T. Tominaga, Tissue factor expression in breast cancer tissues: Its correlation with prognosis and plasma concentration. *Br. J. Cancer* **83**, 164–170 (2000).
62. M. Labelle, R. O. Hynes, The initial hours of metastasis: The importance of cooperative host-tumor cell interactions during hematogenous dissemination. *Cancer Discov.* **2**, 1091–1099 (2012).
63. S. Lucotti *et al*., Aspirin blocks formation of metastatic intravascular niches by inhibiting platelet-derived COX-1/thromboxane A2. *J. Clin. Invest.* **129**, 1845–1862 (2019).
64. J. M. Hou *et al*., Clinical significance and molecular characteristics of circulating tumor cells and circulating tumor microemboli in patients with small-cell lung cancer. *J. Clin. Oncol.* **30**, 525–532 (2012).
65. V. Murlidhar *et al*., Poor prognosis indicated by venous circulating tumor cell clusters in early-stage lung cancers. *Cancer Res.* **77**, 5194–5206 (2017).
66. J. V. Michael *et al*., Platelet microparticles infiltrating solid tumors transfer miRNAs that suppress tumor growth. *Blood* **130**, 567–580 (2017).
67. S. Ito *et al*., A small-molecule compound inhibits a collagen-specific molecular chaperone and could represent a potential remedy for fibrosis. *J. Biol. Chem.* **292**, 20076–20085 (2017).
68. G. Zhang *et al*., Distinct roles for Rap1b protein in platelet secretion and integrin αIIbβ3 outside-in signaling. *J. Biol. Chem.* **286**, 39466–39477 (2011).
69. B. Győrffy *et al*., An online survival analysis tool to rapidly assess the effect of 22,277 genes on breast cancer prognosis using microarray data of 1,809 patients. *Breast Cancer Res. Treat.* **123**, 725–731 (2010).
70. B. P. Zhou, R. Xu, Snail and Twist expression in HMLE and MCF10A cells. Gene Expression Omnibus (GEO). https://www.ncbi.nlm.nih.gov/geo/query/acc.cgi?acc=GSE143349. Deposited 9 January 2020.